AGU PUBLICATIONS

JGR

Journal of Geophysical Research: Biogeosciences

RESEARCH ARTICLE
10.1002/2015JG003097

Key Points:
- PAHs and algal organic matter are well related to air temperature during the past 60 years
- Algal organic matter is suggested to enhance the accumulation of PAHs
- Temperature plays a significant role in increase of algal productivity and PAH deposition

Supporting Information:
- Supporting Information S1

Correspondence to:
Y. Ran,
yran@gig.ac.cn

Citation:
Duan, D., Y. Huang, H. Cheng, and Y. Ran (2015), Relationship of polycyclic aromatic hydrocarbons with algae-derived organic matter in sediment cores from a subtropical region, *J. Geophys. Res. Biogeosci.*, *120*, 2243–2255, doi:10.1002/2015JG003097.

Received 13 JUN 2015
Accepted 11 OCT 2015
Accepted article online 19 OCT 2015
Published online 14 NOV 2015
Corrected 06 JAN 2016

This article was corrected on 06 JAN 2016. See the end of the full text for details.

Relationship of polycyclic aromatic hydrocarbons with algae-derived organic matter in sediment cores from a subtropical region

Dandan Duan[1,2], Youda Huang[1,2], Hefa Cheng[1], and Yong Ran[1]

[1]State Key Laboratory of Organic Geochemistry, Guangzhou Institute of Geochemistry, Chinese Academy of Sciences, Guangzhou, China, [2]University of Chinese Academy of Sciences, Beijing, China

Abstract The influence of algae-derived organic matter (AOM) and climate warming on the historical record of polycyclic aromatic hydrocarbons (PAHs) in the subtropical reservoir sediments was investigated. The profiles of PAH concentrations and AOM contents at the eutrophic and meso-eutrophic reservoirs are significantly elevated and show good correlations with increasing mean air temperature during the past 60 years, suggesting that increasing temperature plays a significant role in increase of algal productivity and PAH deposition. Temperature-mediated AOM is suggested to enhance the deposition and accumulation of pyrogenic PAHs in the sediment cores, also implying an inaccurate estimation on the historical record for atmospheric deposition of PAHs in eutrophic and meso-eutrophic reservoirs. For an oligotrophic reservoir, PAHs decrease as the sediment depth decreases and are less significantly related to AOM. As the oligotrophic reservoir is phosphorus limited and its AOM is significantly oxidized, the effect of increasing temperature on AOM and PAHs is insignificant.

1. Introduction

Reconstruction of the pollution historical record for atmospheric polycyclic aromatic hydrocarbons (PAHs) is important for evaluating regional pollution and for establishing effective pollutant control stipulations. Owing to the lack of historical atmospheric monitoring data, numerous researchers have relied on undisturbed dated sediment cores to reconstruct historical variations of atmospheric contaminants, especially in remote regions [*Fernandez et al.*, 2000; *Muir et al.*, 1996; *Simcik et al.*, 1996; *Yang et al.*, 2010]. In most cases, these variations of contaminants in sediment cores have been attributed to long-range atmospheric transfer and deposition [*Fernandez et al.*, 2000; *Yang et al.*, 2010]. And as a matter of fact, contaminant loadings to water bodies are usually affected by aquatic productivity through the biological pump effect [*Dachs et al.*, 2000; *Duan et al.*, 2014; *Michelutti et al.*, 2009; *Wu et al.*, 2012]. In addition, recent investigations on high-arctic and subarctic lakes suggested that sedimentary accumulation rates of Hg and other organic contaminants may have been closely associated with climate-driven algal productivity [*Carrie et al.*, 2010; *Outridge et al.*, 2005; *Outridge et al.*, 2007; *Stern et al.*, 2009]. However, *Kirk et al.* [2011] on 14 Canadian arctic and subarctic lakes suggested that the relationship between AOM and climate warming was irrelevant. Therefore, the above observations recall for more investigations on the effects of trophic levels, early diagenesis, preservation of organic matter, and oxidation-reduction processes of lakes on the relationship of AOM to climate warming.

Several studies have shown impact of global warming on subtropical lakes in recent years. *Hambright et al.* [1994] investigated how changing temperature affects the thermocline dynamics, such as to prolonged periods of stratification, in a subtropical lake. Changes in thermal stratification in turn might result in large alteration in the phytoplankton community [*Becker et al.*, 2008]. The different phytoplankton assemblages in subtropical lake contain different lipid compositions and concentrations [*Benamotz et al.*, 1985; *Shifrin and Chisholm*, 1981], which might have a strong effect on uptake of hydrophobic pollutants from dissolved phase to particulate phase [*Larsson et al.*, 1998]. Therefore, these findings lead us to hypothesize that phytoplankton in subtropical lakes may experience climate-affected changes, thereby leading to large variations in the transport of hydrophobic contaminant input from the atmosphere to the water column and sediments.

Some remote reservoirs in subtropical area such as the Pearl River Delta (PRD) are well protected and have no point source input of contaminants [*Hua et al.*, 2003; *Lin et al.*, 2007]. Autochthonous primary productivity

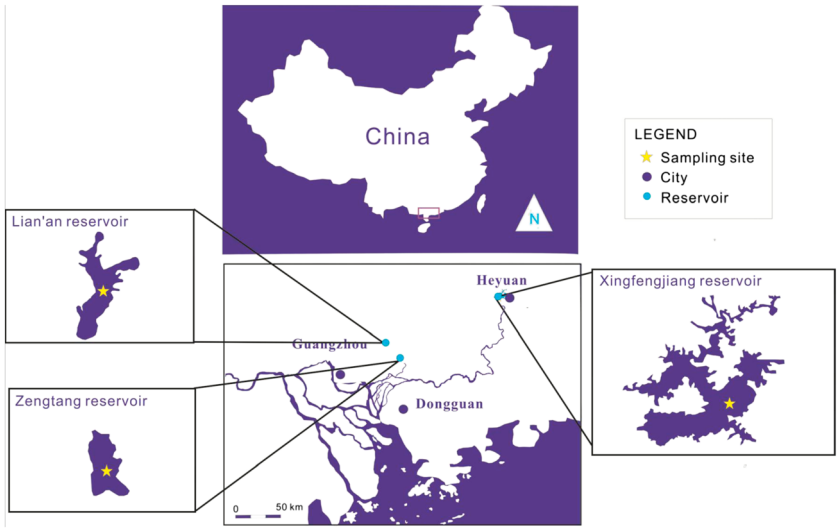

Figure 1. Locations of sampling site in Pearl River Delta.

appears to be the dominant source of organic matter (OM) in the sediment of these remote reservoirs. This OM input can be estimated and identified by Rock-Eval analysis [*Carrie et al.*, 2012; *Disnar et al.*, 2003] and neutral sugar data.

In the present study, three reservoirs within PRD with contrasting hydrologic and trophic levels were selected for examination of the sedimentary record of PAHs over the past 60 years. The AOM in sediments of reservoirs was identified and characterized by the Rock-Eval pyrolysis and neutral sugars data. The relationship between PAHs and AOM in these sediment cores was investigated. The deposition process of PAHs in the reservoirs coupled with climate change was also studied. Lead (Pb) was determined to investigate the extent of anthropogenic influences in these aquatic ecosystems, while aluminum (Al) and iron (Fe) were measured for analyzing the mineral fractions of sediments. The temporal changes of nutrient inputs were reflected by the total nitrogen (TN) and total phosphorus (TP) in sediment cores. To our knowledge, the current investigation represents the first study on the relationship of PAHs with climate-affected algal productivity in a subtropical region.

2. Materials and Methods

Zengtang reservoir (ZT) and Lian'an reservoir (LA) have similar catchment areas and different depths and are located at a distance of 25 km from each other. ZT (23.22°N, 113.76°W) is a shallow, polymictic lake located in the east of Zengcheng and covers a catchment area of 34 km^2. It has a mean depth of 2.5 m and a maximum depth of 5 m. This reservoir was constructed in 1958 and can be classified as a mesotrophic lake before 2003 [*Liu et al.*, 2011]. LA (23.4°N, 113.66°W) is located in the northwest of Zengcheng, which is a monomictic lake with a water area of 43 km^2. A dam, which raised the water level by a maximum of 60 m, was constructed in 1960. This reservoir typically stratifies in the summer and experiences mixing in the winter. It is a meso-eutrophic lake based on the aquatic chemical data. These two reservoirs are mainly fed by precipitation and receive some runoffs from around areas. Xinfengjiang (XFJ) (23.77°N, 114.57°W), built in 1958–1960, is the largest reservoir in Guangdong province and is located near Heyuan. It covers a catchment area of 5730 km^2 and has a storage capacity of 13.98 km^3. The average depth of XFJ is 28.7 m, and the maximum depth is higher than 93 m. It is an oligotrophic and monomictic lake and is thermally stratified throughout much of the year [*Hong et al.*, 2008]. All the three reservoirs are small body of water before the dam constructions. The locations of three reservoirs are shown in Figure 1.

Undisturbed sediment cores were collected in 2010 and 2011 from the central part of the studied lakes using a 6 cm diameter gravity corer with a Plexiglass liner. The core liners were pushed down slowly in order to avoid disturbance. The water depths for the sampling sites at ZT, LA, and XFJ reservoirs are 3 m, 17 m, and 36 m, respectively. The sediment cores were sliced at 2 cm thick intervals using extruding equipment. The

subsamples were immediately placed in plastic bags, sealed, and stored at low temperature (0–10°C) and then were quickly transported to the laboratory, where they were kept at −18°C, freeze-dried and stored until further analysis. The age of each sliced sample was measured by ^{210}Pb and ^{137}Cs radiometric dating.

Detailed descriptions of the analytical procedures including extraction, separation, and analysis of PAHs for the samples are reported elsewhere [*Ma et al.*, 2010; *Mai et al.*, 2002]. GC-MS (Gas Chromatography-Mass Spectrometer) analysis was carried out on an Agilent 6890/5975, (USA) system operating at 70 eV under the selective ion monitoring scan mode. Analytes were separated with a DB5-MS column (30 m × 0.25 mm diameter and 0.25 μm film thickness). Peak confirmation and quantification was performed on a Chemstation system (Agilent).

All the sediments were analyzed by Rock-Eval 6 (Vinci Technologies, France) [*Outridge et al.*, 2005]. This method can determine the quantity and quality of the organic matter in a sample on the basis of the rate of thermal pyrolysis and evolution of various organic compounds. Bulk sediment is first heated in an inert, O_2-free oven (100°C–650°C), followed by combustion in an oxidation oven (400°C–850°C). The pyrolysis stage releases two specific populations of hydrocarbons (HC), defined as S1 and S2, which are detected by a flame ionization detector. Simultaneously, CO and CO_2 detected by infrared detector (milligrams of CO and CO_2 per gram), representing mostly oxygen-bearing OM, is named S3. The combustion stage burns the remaining OM, yielding the refractory carbon (RC, weight percent) peak. Total organic carbon (TOC, weight percent) is the sum of OM from the two steps.

Neutral sugars were separated isocratically using 25 mmol L^{-1} NaOH on a PA1 column in a Dionex 500 system with a pulsed amperometric detector. The procedure of pretreatment of sediment samples was based on *Skoog and Benner* [1997]. The total neutral carbohydrate (TCHO) has been defined as the sum of seven neutral sugars: Glucose (Glu), mannose (Man), galactose (Gal), arabinose (Ara), fucose (Fuc), rhamnose (Rha), and xylose (Xyl).

All the samples for analysis of Pb, Fe, and Al were freeze-dried and completely digested using a mixture of nitric and hydro-fluoric acids and then analyzed by inductively coupled plasma/mass spectrometry (ICP/MS, Agilent 7700X, USA).

The sediment samples from three reservoirs were dated by ^{210}Pb radiometric dating and ^{137}Cs radiometric dating. The activity of ^{210}Pb and ^{137}Cs were measured by S-100 Multi Channel Spectrometer (Canberra, USA) with a PIPS Si detector and a GCW3022 H-P Gecoaxial detector, respectively. Cesium-137 activity was determined using its gamma emission at 661 keV. Excess ^{210}Pb was measured by subtracting the average ^{210}Pb activities of deeper layers. Lead-210 activity data were used for chronological calculation based on a constant rate of supply dating model (CRS) [*Appleby and Oldfield*, 1978]. Cesium-137 activities in sediment cores were calculated based on an apparent peak derived from the nuclear weapon test period in the middle of 1960s [*Ritchie and McHenry*, 1990]. Thus, ^{137}Cs dating method usually is coupled with ^{210}Pb technique to support each other. In this study, the deviation of dating is within the range of 0.01 to 2.3 years.

Total phosphorus (TP) was extracted from sediments with 1 M HCl after ignition of 550°C (2 h) and then determined by a spectrophotometric method with the phosphomolybdenun-blue procedure [*Carnero-Bravo et al.*, 2015; *Páez-Osuna et al.*, 1991]. Total nitrogen (TN) was analyzed by Vario TOC Select: TOC/TN analyzer (Elementar, Germany).

PAHs analyzed in this study were detected well above the quantification limits. Quality assurance for PAHs analyses was provided by analyzing duplicates of an environmental sample, a blank sample, a spiked sample, and a standard reference material (SRM1941, NIST, USA) and by monitoring the recovery of surrogate compounds within each set of environmental samples. Mean percentage of analyte recoveries calculated from surrogate data were 40 ± 9 ($p < 0.05$), 60 ± 7 ($p < 0.05$), 75 ± 9 ($p < 0.05$), 86 ± 7 ($p < 0.05$), and 95 ± 12 ($p < 0.05$) for naphthalene-d8, acenaphthene-d10, phenanthrene-d10, chrysene-d12, and perylene-d12, respectively. Accuracy based on the certified reference material (CRM) was within 5%, and precision was better than 5% of the established values. Final PAH concentrations in this study were not corrected by the recoveries of the surrogate standards. For the Rock-Eval analyses, accuracy and precision were measured by use of the Geological Survey sediment (CFP160000) as a reference standard. Accuracy and precision were within 3% and better than 3% of the established values, respectively. For the neutral sugar analyses, the analytical precision of duplicate samples performed on different days was within ±3% for glucose and ±5% for other sugars. For the Pb, Fe,

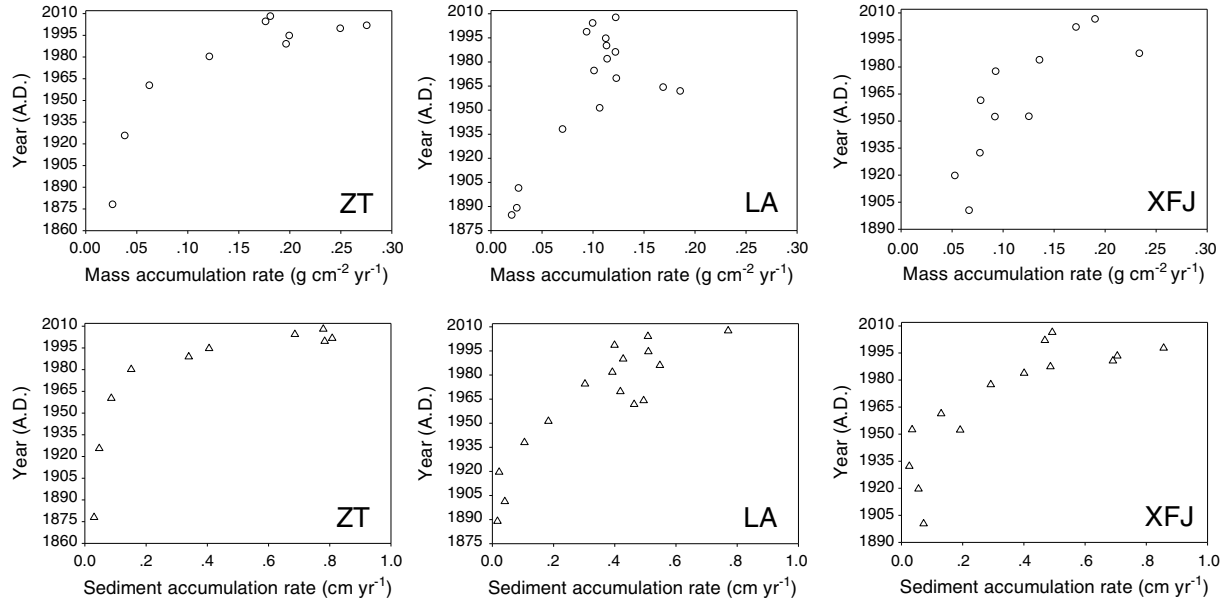

Figure 2. Accumulation rates of ZT, LA, and XFJ cores.

and Al analyses, quality assurance was provided by analyzing a certified reference material (CRM1646a, NIST, USA), an environmental duplicate, and a blank sample for each batch of up to 10 samples. Accuracy and precision were within 5% and better than 5% of the established values, respectively. For TN and TP analyses, the analytical precision of duplicate samples was within ±3.6% for TN and ±5% for TP.

3. Results

3.1. Dating of Sediment Cores

The vertical profiles of ^{137}Cs and ^{210}Pb activities at three reservoirs are shown in Figure S1 in the supporting information. Ages and sedimentation rates were estimated from ^{210}Pb activity (half-life 22.23 years) by using the CRS (constant rate of supply) model [*Sanchez-Cabeza and Ruiz-Fernández*, 2012]. To check the ^{210}Pb dates, the samples were also analyzed for ^{137}Cs activity (half-life 30.17 years), which shows the maximum value in accordance with the significant ^{137}Cs event of nuclear weapon testing in 1963 [*Ritchie and McHenry*, 1990].

The results of the CRS model for ^{210}Pb dating are shown in Figure 2. Sediment accumulation rates vary from 0.03 to 0.81 cm a^{-1}, from 0.04 to 0.77 cm a^{-1}, and from 0.06 to 0.86 cm a^{-1} in the sediment cores at ZT, LA and XFJ, respectively, with mass accumulation rates in the ranges of 0.03–0.28 g cm^{-2} a^{-1}, 0.02–0.19 g cm^{-2} a^{-1}, and 0.05–1.07 g cm^{-2} a^{-1}. The ^{210}Pb dates are in good agreement with the ^{137}Cs dates (Figure 2). For example, the ZT, LA, and XFJ cores give apparent peaks of ^{137}Cs activity (6.9 Bq kg^{-1} at 21 cm depth of ZT core; 23.3 Bq kg^{-1} at 19 cm depth of LA core; 30.3 Bq kg^{-1} at 22 cm depth of XFJ core) corresponding to A.D. 1961, 1964 and 1962, respectively. In this study, the deviation of dating is within the range of 0.5 to 2.3 years for^{210}Pb technique.

3.2. Parameters of OM in the Sediment Cores

TOC, S1, S2, Hydrogen Index (HI), and Oxygen Index (OI) were determined by Rock-Eval pyrolysis. TOC ranges from 0.78% to 3.38% in ZT core, from 0.88% to 4.3% in LA core, and from 0.47% to 1.76% in XFJ core. For ZT and LA cores, S1 values are respectively in the ranges of 0.13–1.31 mg HC/g and 0.21–1.32 mg HC/g, while S2 values are respectively in the ranges of 1.10–8.38 mg HC/g and 1.47–9.45 mg HC/g, showing increasing trends from the bottom layers to the top sections. On the contrary, S1 (0.10–0.33 mg HC/g) and S2 (0.73–2.78 mg HC/g) respectively illustrate a decreasing trend toward the top layers in XFJ core (Table S1 in the supporting information). It is found that all organic matter fractions are highly correlated with each other (For ZT, S1:S2 $R^2 = 0.98$, S2:RC $R^2 = 0.95$, S2:TOC $R^2 = 0.98$, $p < 0.01$; For LA, S1:S2 $R^2 = 0.99$, S2:RC $R^2 = 0.93$, S2:TOC $R^2 = 0.94$, $p < 0.01$; For XFJ, S1:S2 $R^2 = 0.99$, S2:RC $R^2 = 0.97$ S2:TOC $R^2 = 0.96$, $p < 0.01$).

Mineral carbon (inorganic carbon) obtained from Rock-Eval pyrolysis is in the range of 0.18–0.38%, 0.11–0.40%, and 0.18–0.47% in ZT, LA and XFJ sediment cores, respectively (Figure S6 in the supporting information).

The hydrogen index (HI) and oxygen index (OI) are presented in Table S1, which are calculated by normalizing the contents of S2 and S3 to total organic carbon [*Stern et al.*, 2009]. The HI values in ZT, LA, and XFJ cores range from 114 to 248 mg HC/g TOC, from 151 to 229 mg HC/g TOC, and from 141 to 196 mg HC/g TOC, respectively. The HI values in each of the sediment cores show an increasing trend from the bottom to the top layers. The OI values in XFJ core (375–883 mg CO_2/g TOC) are higher than in ZT core (220–524 mg CO_2/g TOC) and LA core (254–397 mg CO_2/g TOC).

TP concentrations in ZT and LA sediment cores vary from 0.02 to 0.12 mg/g and from 0.03 to 0.15 mg/g, respectively, which are higher than those in XFJ sediment core (0.005–0.037 mg/g). TN contents in ZT and LA cores are respectively in the range of 0.20–0.41% and 0.09–0.41% and are also higher than those in XFJ core (0.19–0.29%) (Figure S6). Al concentrations in ZT, LA, and XFJ cores respectively range from 3.1% to 5.8%, from 1.9% to 10.5%, and from 3.7% to 10.3%, whereas Fe concentrations are in the range of 0.43%–0.84%, 0.3%–1.3%, and 0.7%–1.2%, respectively (Figure S6). As shown in Figure 4, the TCHO values in each of the ZT, LA, and XFJ cores show a significant increase from the bottom to the surface, ranging from 1.94 to 5.36 mg/g, 0.51 to 6.4 mg/g, and 0.83 to 2.56 mg/g, respectively.

3.3. Historical Variation of PAHs

As the recovery of naphthalene-d8 was only about 40%, it was excluded from the data analysis. The total PAH concentrations are the sum of 15 U.S. EPA priority PAHs. All total PAH concentrations are based on dry weight and are shown in Table S1 in the supporting information. The concentrations of PAHs in ZT, LA, and XFJ cores are in the ranges of 69–376 ng/g, 63–355 ng/g, and 38–405 ng/g, respectively, with the mean concentrations of 167 ng/g, 197 ng/g, and 179 ng/g (Figure 4 and Table S1). ZT and LA similarly exhibit considerable increases in PAH concentrations from the bottom to the top of the sediment cores. For XFJ, PAH concentrations gradually decrease in the sediment core since 1950 except for two intervals during 1969–1981 and 1986–1995.

3.4. Temperature Data

The meteorological data were obtained from several fiducial stations, which are built for monitoring climate change in a very broad area and are different from the weather stations designed for city weather report. The trends are plotted in Figures 6a–6d. The mean air temperature in the Guangzhou area has increased by about 1.5°C since 1970 (Figure 6a) but shows significant historical low values around 1970, 1986, and 1996. And the mean air temperature in the Heyuan area has increased by about 1.52°C between 1957 and 2004 (Figure 6c). Therefore, the above evidence supports an overall climate warming during the last six decades.

4. Discussions

4.1. OM Input and Variation in the Sediment Cores

Rock-Eval analysis is a traditional analytical technique in petroleum geochemistry. This rapid, efficient technique has been demonstrated to be suitable for organic matter characterization [*Duan et al.*, 2014; *Sanei et al.*, 2005; *Stern et al.*, 2009]. Although this simple method for specific assessment of algal-derived OM in recent sediments is still questionable, it has been increasingly applied to bulk sediments during the last decade. Especially the signal S2 from the pyrolysis process has been shown to represent algal-like macromolecular organic matter and to be more resistant to degradation than other organic fractions during early diagenesis. In this study, it is found that all organic matter fractions (S1, S2, S3, RC, and TOC) are highly correlated with each other, indicating that the different organic compartments may originate from the same source or have undergone the similar geochemical processes. Moreover, planktonic algae (e.g., green algae and diatom) is the primay producer in these investigated reservoirs. Therefore, the enhanced algal production could play an important role to sediment TOC and lead to the significant increase in the sedimentary organic matter during the last decades.

The hydrogen index (HI) and oxygen index (OI) (Table S1) as well as the ratio of HI to OIRE6 can provide more evidences for the source of organic matter [*Whelan and Thompson-Rizer*, 1993]. Especially the HI index was observed to be a good proxy for the lacustrine productivity in an investigation on NOM (natural organic matter) in different trophic lakes [*Bechtel and Schubert*, 2009]. In immature sediments, an HI value lower than 100 mg HC/g TOC indicates a dominantly terrigenous (higher plant) source of the organic matter, whereas an HI value

higher than 100 mg HC/g TOC indicates a dominant contribution of aquatic algae and/or microbial biomass [*Meyers*, 1997; *Stein et al*., 2006]. All the samples in this study are immature sediments and their HI values are above 100 mg HC/g TOC, and the profiles of HI have similar trends (Figure 4), suggesting a dominant algal source to the sediments in the three reservoirs. The HI values are arranged in the sequence: 248 > 229 > 194 mg HC/g TOC in the surface sediments of LA, ZT, and XFJ, which is the same as the sequence of chlorophyll a values: 90.7 > 21.2 > 1.1 μg/L [*Duan et al*., 2014]. In addition, the HI values in the ZT, LA, and XFJ reservoirs are higher than those in the algae-dominated Kusawa Lake sediments (62–121 mg HC/g TOC) [*Stern et al*., 2009] in Canada. Moreover, the OI values at ZT (220–524 mg HC/g TOC) and LA (254–397 mg HC/g TOC) are a little lower than at XFJ (375–883 mg HC/g TOC) and Kusawa Lake (336–822 mg HC/g TOC) [*Stern et al*., 2009]. Furthermore, the HI/OIRE6 ratios at ZT (0.30–1.85) and LA (0.46–0.95) are higher than at XFJ (0.20–0.53) and Kusawa Lake (0.13–0.36). Although the HI/OIRE6 ratios at these two reservoirs are not consistent with a criteria obtained from biological standards of phytoplankton (HI/OIRE6 > 2) [*Carrie et al*., 2012], they are higher than in the arctic algae-dominated Kusawa Lake. Thus, the Rock-Eval parameters (e.g., S2, HI) can be used as AOM indicators and provide important information on primary productivity in these aquatic ecosystems.

The decreasing trends for S1, S2, and TOC from the bottom to the top sediment core at XFJ (Table S1) suggest that NOM in this oligotrophic reservoir, where primary productivity is low and dissolved oxygen concentrations are high, might experience a higher degree of degradation and oxidation than at ZT and LA (Table S1). Moreover, the TOC concentrations at XFJ are highest prior to construction of the reservoir, which is related to the fact that this site was previously a much smaller body of water, and hence more like the ZT reservoir. Nutrient concentrations and light penetration would presumably have been much larger in such a system, thus providing a greater algal biomass. After the dam was constructed, we hypothesized that decreasing OM production was caused by a variety of ecological processes (e.g., lower light penetration from deeper water yielding lower photosynthesis, lower concentration of nutrients) in the large XFJ reservoir. In support of this hypothesis, the color of the XFJ sediment core is very different from that in the ZT or LA core. The sediments are brown-black at ZT and LA but yellow at XFJ, suggesting that the former sediments are anoxic and the latter one is oxic. Therefore, the decreasing NOM after the dam construction at XFJ could be attributed to low primary productivity and/or bacterially mediated oxidation of NOM.

The sedimentary record of the S2 fraction could be affected by inputs of terrestrial (i.e., higher plant) organic matter and inorganic clastic material. Refractory carbon (RC), which partially represents the thermally resistant organic material, mainly originates from terrestrial organic matter (e.g., lignin and cellulose) and hence can be used to reflect terrestrial input [*Lafargue et al*., 1998]. However, variations of major algae-derived OC (S1 and S2) are highly correlated ($p < 0.001$) with those RC in each of the three reservoirs, suggesting that terrestrial source of organic matter is negligible. If there is a terrestrial input of organic matter, the RC fractions would disproportionately increase relative to the other organic compartments.

Early diagenesis of organic matter after the deposition needs to be taken into consideration for correctly understanding the proxies of productivity (e.g., S2 and HI) in aquatic ecosystems. The S2 fraction is demonstrated to be resistant to degradation and is similar to the algaenan and nonhydrolytic nonprotein alkyl carbons in sediments [*Ran et al*., 2007; *Sanei et al*., 2005]. It was observed that the degradation of nonhydrolytic nonprotein alkyl carbons was significantly related to oxygen exposure time in the marine sediments [*Gélinas et al*., 2001]. According to their observation, it is estimated that the S2 fraction would be degraded by 5% during 1000 years. Moreover, the profiles of neutral sugar compositions and the weight percent $(Fuc + Rha)_b$ values were relatively stable in the sediment cores, and there is no significant decline in weight percent glucose with depths in these cores (D. Duan et al., unpublished data, 2016). Hence, it is suggested that the degradation of NOM in the sediment cores is not significant after the deposition. Furthermore, *Outridge et al*. [2007] used the patterns of S2/RC ratios in a sediment core to analyze the effect of diagenesis on the S2 signal. In our study, the S2/RC profiles at ZT and XFJ exhibit gradually declining trends from the top to the bottom of the cores (Figure S2, supporting information). The dominant algal organic matter input is likely to be responsible for the trend at ZT because the primary production has been enhanced since 2003 [*Liu et al*., 2011]. But S2 at XFJ may suffer from decomposition (see the above discussion) [*Lin et al*., 2007]. At LA, a relative stable S2/RC profile is present over most of the core (from 34 cm to 10 cm; Figure S2 in the supporting information). The sharp increase in S2/RC above about 8 cm indicates the change of primary productivity (Figure S2, supporting information). In general, it is concluded that the S2 signals for the LA and ZT sediment cores are well preserved and appear to mainly originate from autochthonous primary productivity.

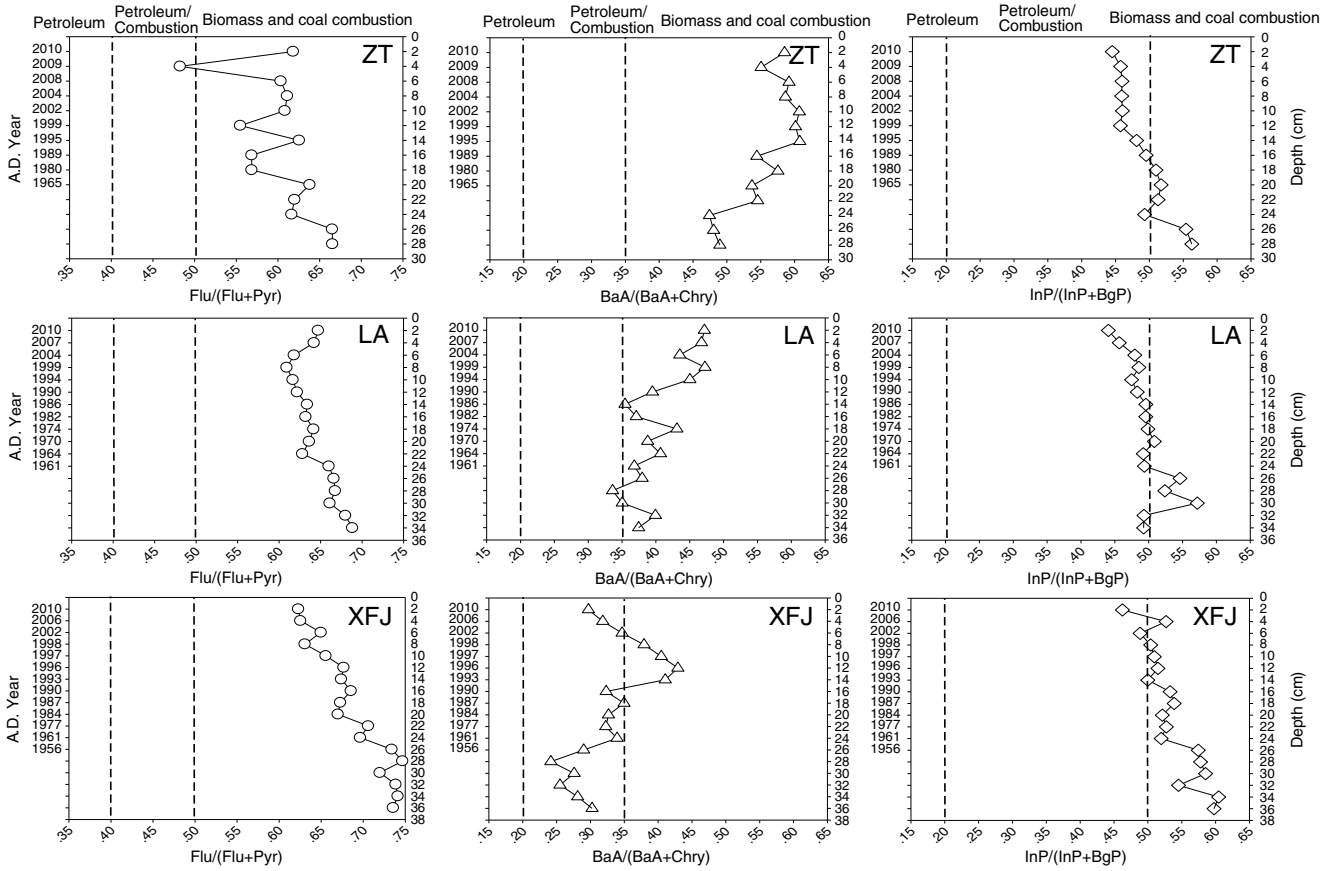

Figure 3. Temporal trends of PAHs ratios in ZT, LA, and XFJ cores.

4.2. Historical Changes in the Source and Deposition of PAHs

Three PAH isomer ratios, i.e., benzo(a)anthracene/(benzo(a)anthracene + chrysene) (BaA/(BaA + Chry)), fluoranthene/(fluoranthene + pyrene) (Fla/(Fla + Pyr)), and indene(1,2,3-c,d)pyrene/(indene(1,2,3-c,d)pyrene + benzo(g,h,i)perylene) (InP/(InP + BghiP)) were used to identify the different sources of PAHs at the ZT, LA, and XFJ reservoirs. The criteria for the source identification are as follows: (a) Fla/(Fla + Py) ratio < 0.40 indicates dominance of petroleum, 0.40–0.50 indicates petroleum combustion, and > 0.50 combustion of coal, grasses, and wood; (b) BaA/(BaA + Chry) ratio < 0.20 indicates petroleum, 0.20–0.35 petroleum and combustion, and > 0.35 combustion; (c) InP/(InP + BghiP) < 0.20 indicates petroleum, 0.20–0.50 petroleum combustion, and > 0.50 combustion of coal, grasses, and wood [*Yunker et al.*, 2002]. PAH ratios and their temporal variations were shown in Figures 3 and S3 in the supporting information, respectively.

The profiles of Fla/(Fla + Pyr) ratios showed similar trends decreasing toward to the top sections of sediment cores at ZT, LA, and XFJ, but all their values were much higher than 0.5 (Figure 3). These values suggest that PAHs at ZT, LA, and XFJ were derived mostly from biomass and coal combustion, rather than from unburned petroleum, and only one sample showed petroleum combustion source. In addition, the vertical changes of BaA/(BaA + Chry) ratios also confirm the above results at ZT, and LA and showed the predominance of biomass and coal combustion sources. However, the BaA/(BaA + Chry) ratios indicate major sources from petroleum combustion at XFJ before 1992. The profiles of BaA/(BaA + Chry) ratios in this study did not show a shift (from petrogenic ($<$0.2) to pyrogenic PAHs ($>$0.2)) as described in the literature [*Louchouarn et al.*, 2012], further suggesting that biomass, coal, and petroleum combustion are the main sources of PAHs in the reservoirs.

InP/(InP + BghiP) ratios were different from Fla/(Fla + Pyr) ratios and BaA/(BaA + Chry) ratios. PAHs in most samples were derived from petroleum combustion as suggested by the values of InP/(InP + BghiP) ratios, which were slightly smaller than 0.5 (Figure 3). Thus, PAHs in the studied areas may be originated partly from vehicle emission and fossil fuel combustion and were mixed with the biomass and coal combustion sources.

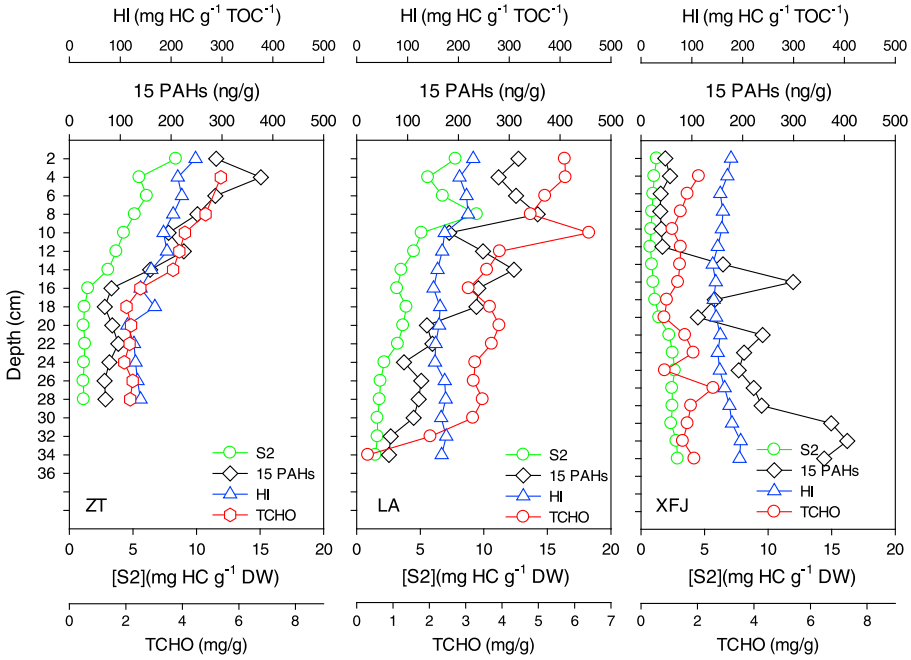

Figure 4. Point-by-point comparison between PAHs, HI, S2, and TCHO concentrations in the sediment cores of three reservoirs.

Moreover, methyl-phenanthrenes/phenanthrene (MP/P) ratio has been frequently used to differentiate petrogenic and pyrogenic PAHs [*Zakaria et al.*, 2002]. The MP/P ratio typically ranges from 2 to 6 for unburned fossils but is generally <1 for combustion residues. In this study, MP/P ratios at ZT and LA were <1, confirming the above conclusion that PAHs were mostly derived from coal, grass, and wood combustion in these regions. The major pathway for the input of PAHs to the reservoirs is atmospheric deposition.

ZT and LA similarly exhibited considerable increases in PAHs from the bottom to the top of the sediment cores, which are consistent with other investigations [*Liu et al.*, 2012; *Mai et al.*, 2001]. But these investigations only attributed the elevated PAHs in the sediment cores to the increasing emission of PAHs. As mentioned in section 1, contaminant loadings to water bodies are usually affected by aquatic productivity through the biological pump effect [*Dachs et al.*, 2000; *Duan et al.*, 2014; *Michelutti et al.*, 2009; *Wu et al.*, 2012]. Recent investigations on high-arctic and subarctic lakes suggested that sedimentary accumulation rates of Hg and other organic contaminants may have been closely associated with climate-driven algal productivity [*Carrie et al.*, 2010; *Outridge et al.*, 2005; *Outridge et al.*, 2007; *Stern et al.*, 2009]. Hence, the enriched PAHs in the three sediment cores may be not only affected by the extent of atmospheric deposition but also enhanced by inner biogeochemical processes such as tropic level in the reservoirs. In that case, PAHs concentrations have usually been normalized by the TOC for correctly reconstructing the historical record of atmospheric PAH depositions [*Guo et al.*, 2011]. As shown in Figure S4, TOC-normalized PAH concentrations display different trends from the profiles of absolute PAH concentrations (Figure 4) in the reservoirs cores. For example, the higher PAH contents (318 ng/g at 0–2 cm depths; 356 ng/g at 7–8 cm depths) correspond to the lower TOC-normalized PAH concentrations (9.3 μg/g at 0–2 cm depths; 8.2 μg/g at 7–8 cm depths) in the LA core, suggesting the PAHs contents in sediments were significantly enhanced by OM or AOM even though the absorption ability of per unit OM was relatively small. However, considering the diversity effects of different types of algae-derived OM on absorption of PAHs during settling [*Larsson et al.*, 1998], the estimation for atmospheric PAHs deposition is still inaccurate.

Changes in sediment texture (e.g., mineral fractions) could be another possible factor controlling the accumulation of PAHs in sediments. Al has been usually used as a proxy for the granular variations of the aluminosilicate fraction (clays) [*Loring and Rantala*, 1992], as Fe or Al is a major constituent of a large variety of mineral structures such as feldspars, clay minerals, and amorphous aluminosilicate gels [*Bortleson and Lee*, 1972]. In this study, most of the sediments show high contents of clays (mostly >90%). However, Al, Fe, and mineral carbon (%) have no or weak correlation with PAH concentrations in any of the reserovir cores (Table S2 in the

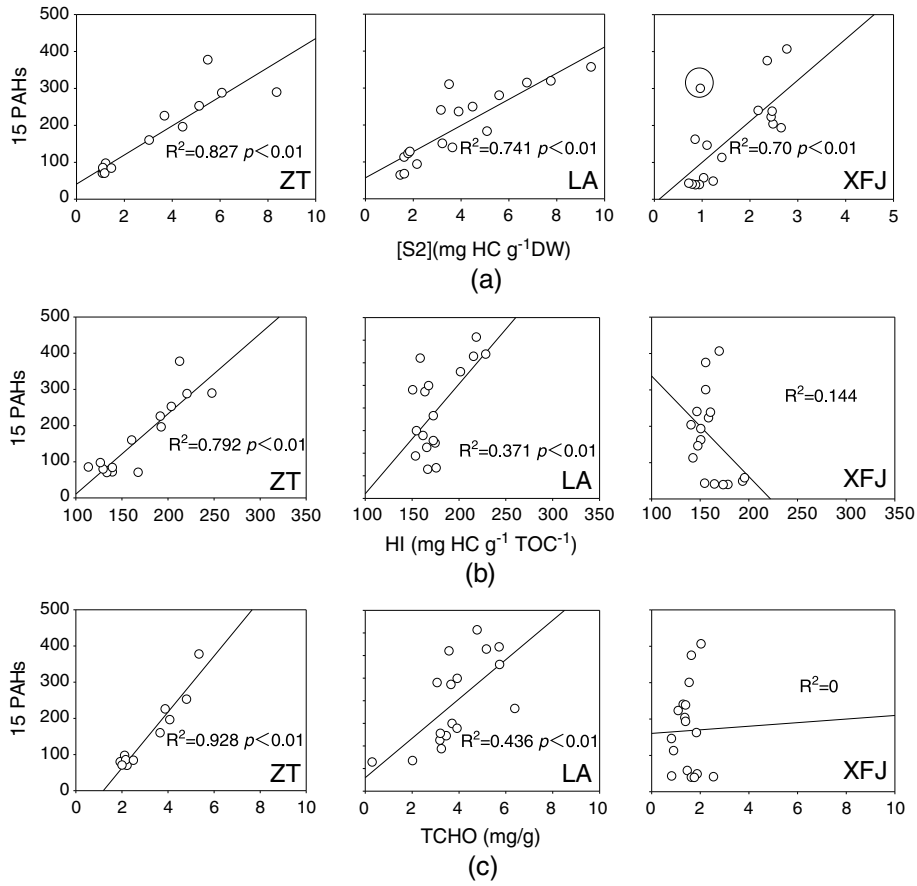

Figure 5. (a) Regression lines between 15 PAHs and S2 in three reservoirs; (b) regression lines between 15 PAHs and HI in three reservoirs. (c) Regression lines between 15 PAHs and TCHO in three reservoirs. Circle indicates an outlier point.

supporting information), suggesting the PAH concentratrions are not influenced by the mineral clays or inorganic carbon in the sediments.

At last, it is necessary to evaluate the extent of surrounding natural and anthropogenic influences on the studied reservoirs for the possible direct input of pollutants from nearby areas. First, the three reservoirs have been well protected during the recent years since the dams were constructed. Second, as the Pb profiles at the three sediment cores did not show enrichment throughout the cores (Figure S5, supporting information), and the Pb concentrations ranging from 4.7 mg kg^{-1} to 20.6 mg kg^{-1} were below the soil background value of Guangdong (23.4 mg kg^{-2}), anthropogenic Pb did not significantly affect the three reservoirs over the last 60 years. To some extent, this provided an evidence that these reservoirs were not heavily affected by surrounding runoffs and nearby anthropogenic activities.

4.3. Relationship Between PAHs and Proxies of Primary Productivity

The vertical profiles of S2, HI, TCHO, and PAHs show marked similarities in both ZT and LA cores (Figure 4). Especially there are apparent links among PAHs, S2, HI, and TCHO in the upper layers of ZT core (3–23 cm) (Table S1 and Figure 4). For the XFJ core, the trends of S2 and PAHs with depths are similar but somewhat more variable and show a peak at depths of 11–20 cm, whereas the vertical profiles of HI and TCHO also show some significant similarities. It is suggested that in the XFJ reservoir algal productivity may also increase relative to the TOC input during the recent years. In the ZT core, the positive correlations between PAHs and S2 ($R^2 = 0.827$, $p < 0.01$) are slightly stronger than those between PAHs and HI ($R^2 = 0.792$, $p < 0.01$) and a little bit weaker than those between PAHs and TCHO ($R^2 = 0.928$, $p < 0.01$). For LA, PAHs show positive correlation with S2 ($R^2 = 0.741$, $p < 0.01$), HI ($R^2 = 0.371$, $p < 0.01$), and TCHO ($R^2 = 0.436$, $p < 0.01$), even though latter two are relatively low (Figure 5 and Table S2). The above correlations suggest that the inputs

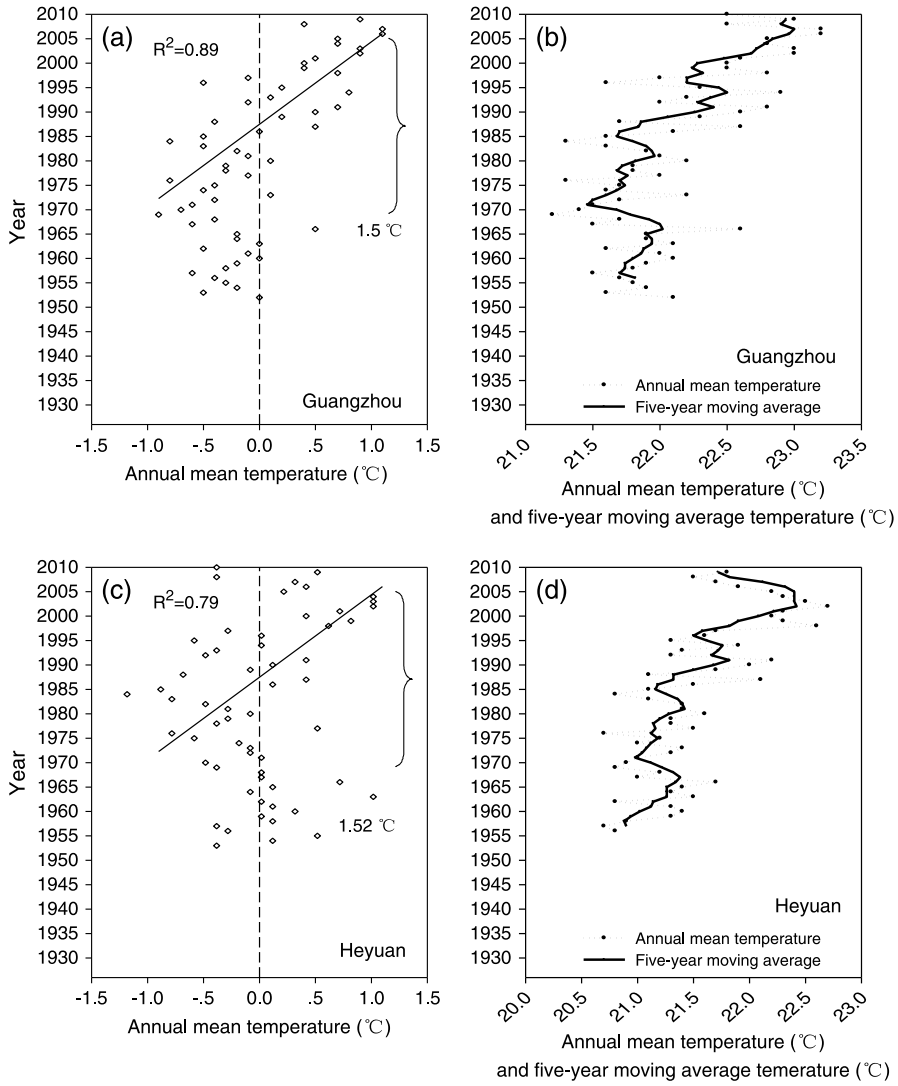

Figure 6. Lake cores (a) annual mean air temperature at Guangzhou area; (b) annual mean temperature and 5 year moving average (T_5) at Guangzhou area; (c) annual mean air temperature at Heyuan area; (d) annual mean temperature and 5 year moving average at Heyuan area. A significant increase in air temperature was observed in the period of 1971 to 2010 at Guangzhoua area ($y = 0.0378x - 52.827$; $R^2 = 0.89$) and in the period of 1957 to 2004 at Heyuan area ($y = 0.0249x + 20.817$; $R^2 = 0.72$).

of PAHs to those sediments are related to algae-derived organic matter. For XFJ, the correlation coefficient between PAHs and S2 is 0.70 ($p < 0.01$), excluding the 15 cm sample. This abnormal point is likely to be caused by redox change or terrestrial input change. The profile of Mn or Fe shows important oxidation and reduction boundary at 23–24 cm in this lake [*Duan et al.*, 2014]. The two lower concentrations of Pb at 15–16 cm and 27–28 cm depth were related with the two lowest water levels recorded in 1980 and 1964, respectively [*Duan et al.*, 2014]. In addition, the water runoff at XFJ had been reduced since the 1970s due to the other reservoir construction in the upstream or the global change, as the flood discharge gate had not been used any more since then. The above fact indicates that, even in this oligotrophic lake, the algal primary productivity is the primary factor in controlling the deposition and preservation of PAHs.

4.4. Effects of Climate Change on Primary Productivity and Accumulation of PAHs

Several studies have shown that climate warming has resulted in significant increases in the sea surface temperature of the South China Sea during the recent decades [*He and Guan*, 1999; *Li et al.*, 2002]. However, the effect of climate warming in subtropical lakes and reservoirs has not been investigated. We examined this effect using the annual average air temperature and 5 year moving averages of the air

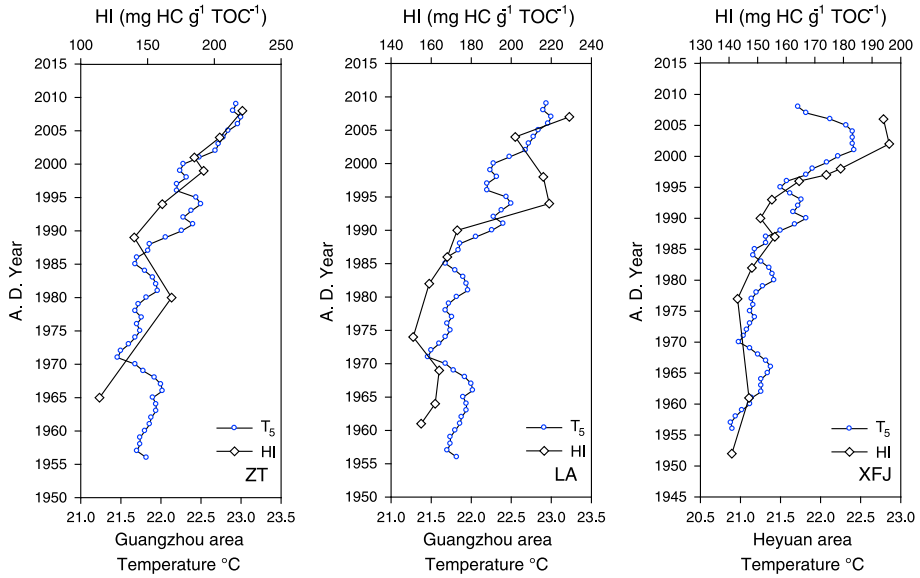

Figure 7. Temporal profiles of 5 year moving temperature (T_5) and hydrogen Index (HI) in sediment cores from three reservoirs.

temperature (T_5) on the time scale of 60 years in the Guangzhou area and Heyuan area, which were obatined from the China Meterological Data Sharing Service System (CMDSSS) for the Guangzhou station (23.10°N, 113.20°W) and the Heyuan station (23.44°N, 114.41°W).

The annual mean temperature and T_5 over 60 years are compared with the profiles of PAHs and S2 in the three revservoirs in Figure 6 and Table S2. The PAHs and S2 profiles at ZT and LA respectively show a good correlation with increasing mean air temperature during the past 60 years, suggesting that climate warming affects autochthonous primary productivities (S2) and, in turn, the deposition of hydrophobic contaminants (PAHs) to the sediments (Table S2). For XFJ reservoir, the profiles of PAHs and S2 show a negative correlation with the temperature variations in this area. As the XFJ reservoir has larger catchment area and deeper water level than the LA reservoir does, it is significantly affected by a limited phosphorus input [*Lin et al.*, 2007] and is likely to be insensitive to the effect of global change on primary productivity during the last 60 years.

As small shallow reservoirs such as ZT generally respond quickly to rainfall, the transport distances and residence times of suspended particles are usually short. High sedimentation rates lead to rapid burial in the sediments, but resuspension and diagenesis processes are usually enhanced [*Benamotz et al.*, 1985]. However, in large and deep water reservoirs like LA and XFJ, as the residence time for suspended particles is on the scale of weeks to as much as a year [*Larsson et al.*, 1998], the resuspension is low due to low physical disturbation. The diagenesis process may also be low when the sediment profile is in anoxic condition. As the surface sediment at LA is in anoxic condition, their AOM are well preserved, and the HI/OI ratios are low. Moreover, the climate-affected primary productivity shows a significant role on the amount of aliphatic carbon, as observed by other investigations in the laboratory [*Becker et al.*, 2008; *Feng et al.*, 2008]. Therefore, the effect of climate warming on autochthonous primary productivity in the sediments of ZT and LA is significant, as observed in other investigations [*Carvalho and Kirika*, 2003; *Gerten and Adrian*, 2000; *Jackson et al.*, 2007].

In addtion, the influence of nutrient inputs on the enhancement of primary productivity needs to be taken into consideration for correctly evaluating the climate effects on primary productivity in reservoirs [*Carnero-Bravo et al.*, 2015]. In general, TP and TN concentrations show overall increasing trends toward to the surficial layers in the ZT and LA cores (Figure S6), whereas they are variable throughout the XFJ core. However, their correlations with HI in the ZT, LA, and XFJ cores are weaker than the correlations of T_5 with HI (Table S2). Moreover, the TP and TN concentrations remained low level (mostly TP < 0.1 mg/g, TN $< 0.4\%$) (Figure S6) during the past decades and are far smaller than those in sediments of other eutrophic reservoirs (TP: 0.3–0.83 mg/g, TN: 0.2–0.9% for Valle de Bravo Lake; TP: 0.55–0.99 mg/g for Qingcaosha reservoir) [*Carnero-Bravo et al.*, 2015; *Jin et al.*, 2013], suggesting the nutrient enrichment in ZT and LA cores either

partially contributes to the productivity enhancement or is associated with climate change as the essential nutrient for algae growth. Thus, the nutrient input is not the key factor affecting the primary productivity in the three reservoirs.

Temporal variations of the T_5 and HI parameters during the last 60 years are plotted in Figure 7. Strong positive correlations between the moving temperature T_5 and HI (S2/TOC*100) are observed at ZT, LA, and XFJ reservoirs. Though the TOC and S2 profiles respectively decline with the increasing temperature at XFJ reservoir due to phosphorus limited, the S2 profile has still increased relative to the decreasing TOC profile from the bottom to the top, suggesting that algal-derived organic matter (S2) is significantly affected by the temperature change at XFJ reservoir during the last decades. As demonstrated above, HI is an important indicator of aquatic productivity in this study. Therefore, the above results suggest that the primary production in ZT, LA, and XFJ reservoirs is strongly associated with climate warming in subtropical area, which is also supported by the results of the Pearson correlation analysis among the T_5, HI, S2, and PAHs (Table S2, supporting information).

5. Conclusions

The historical variations of PAHs in sediment cores from subtropical reservoirs showed a significant relationship with climate-enhanced algal organic matter concentrations. Elevated productivity resulted in increasing algal-derived organic matter, and then accumulated more PAHs in aquatic ecosystem in subtropical reservoirs. It is for the first time found that even at low latitude, the primary productivity in subtropical reservoirs was significantly affected by climate warming, which had been observed in the arctic and subarctic areas. This investigation would help to better assess the accumulation and preservation of PAHs following deposition in this area.

Acknowledgments

Data supporting Figures 2–5 are available as in Tables S1 and S2 in the supporting information. The annual average air temperature and 5 year moving averages of the air temperature on the time scale of 60 years in the Guangzhou area and Heyuan area were obtained from the China Meterological Data Sharing Service System (CMDSSS). This study was supported by a key project of NNSFC-Guangdong (U1201235) and a project of National Natural Science Foundation of China (41473103), and a Key Field Project, Chinese Academy of Sciences (Y234081A07). This is contribution IS-2155 from GIGCAS.

References

Appleby, P. G., and F. Oldfield (1978), The calculation of lead-210 dates assuming a constant rate of supply of unsupported ^{210}Pb to the sediment, *Catena*, *5*(1), 1–8.

Bechtel, A., and C. J. Schubert (2009), A biogeochemical study of sediments from the eutrophic Lake Lugano and the oligotrophic Lake Brienz, Switzerland, *Org. Geochem.*, *40*(10), 1100–1114.

Becker, V., V. L. M. Huszar, L. Naselli-Flores, and J. Padisak (2008), Phytoplankton equilibrium phases during thermal stratification in a deep subtropical reservoir, *Freshwater Biol.*, *53*(5), 952–963.

Benamotz, A., T. G. Tornabene, and W. H. Thomas (1985), Chemical profile of selected species of microalgae with emphasis on lipids, *J. Phycol.*, *21*(1), 72–81.

Bortleson, G. C., and G. F. Lee (1972), Recent sedimentary history of Lake Mendota, Wis, *Environ. Sci. Technol.*, *6*(9), 799–808.

Carnero-Bravo, V., M. Merino-Ibarra, A. C. Ruiz-Fernández, J. A. Sanchez-Cabeza, and B. Ghaleb (2015), Sedimentary record of water column trophic conditions and sediment carbon fluxes in a tropical water reservoir (Valle de Bravo, Mexico), *Environ. Sci. Pollut. Res.*, *22*(6), 4680–4694.

Carrie, J., F. Wang, H. Sanei, R. W. Macdonald, P. M. Outridge, and G. A. Stern (2010), Increasing contaminant burdens in an Arctic fish, Burbot (Lota lota), in a warming climate, *Environ. Sci. Technol.*, *44*(1), 316–322.

Carrie, J., H. Sanei, and G. A. Stern (2012), Standardisation of Rock-Eval pyrolysis for the analysis of recent sediments and soils, *Org. Geochem.*, *46*, 38–53.

Carvalho, L., and A. Kirika (2003), Changes in shallow lake functioning: Response to climate change and nutrient reduction, *Hydrobiology*, *506*(1–3), 789–796.

Dachs, J., S. J. Eisenreich, and R. M. Hoff (2000), Influence of eutrophication on air-water exchange, vertical fluxes, and phytoplankton concentrations of persistent organic pollutants, *Environ. Sci. Technol.*, *34*(6), 1095–1102.

Disnar, J. R., B. Guillet, D. Keravis, C. Di-Giovanni, and D. Sebag (2003), Soil organic matter (SOM) characterization by Rock-Eval pyrolysis: Scope and limitations, *Org. Geochem.*, *34*(3), 327–343.

Duan, D. D., Y. Ran, H. F. Cheng, J. A. Chen, and G. J. Wan (2014), Contamination trends of trace metals and coupling with algal productivity in sediment cores in Pearl River Delta, South China, *Chemosphere*, *103*, 35–43.

Feng, X. J., A. J. Simpson, K. P. Wilson, D. D. Williams, and M. J. Simpson (2008), Increased cuticular carbon sequestration and lignin oxidation in response to soil warming, *Nat. Geosci.*, *1*(12), 836–839.

Fernandez, P., R. M. Vilanova, C. Martinez, P. Appleby, and J. O. Grimalt (2000), The historical record of atmospheric pyrolytic pollution over Europe registered in the sedimentary PAH from remote mountain lakes, *Environ. Sci. Technol.*, *34*(10), 1906–1913.

Gélinas, Y., J. A. Baldock, and J. I. Hedges (2001), Organic carbon composition of marine sediments: Effect of oxygen exposure on oil generation potential, *Science*, *294*(5540), 145–148.

Gerten, D., and R. Adrian (2000), Climate-driven changes in spring plankton dynamics and the sensitivity of shallow polymictic lakes to the North Atlantic Oscillation, *Limnol. Oceanogr.*, *45*(5), 1058–1066.

Guo, J., Z. Liang, H. Liao, Z. Tang, X. Zhao, and F. Wu (2011), Sedimentary record of polycyclic aromatic hydrocarbons in Lake Erhai, Southwest China, *J. Environ. Sci.*, *23*(8), 1308–1315.

Hambright, K. D., M. Gophen, and S. Serruya (1994), Influence of long-term climatic changes on the stratification of a subtropical, warm monomictic lake, *Limnol. Oceanogr.*, *39*(5), 1233–1242.

He, Y. H., and C. H. Guan (1999), A primary study of the South China Sea warm pool, *Plateau Meteorol.*, *18*(4), 595–602.

Hong, H. C., M. H. Wong, A. Mazumder, and Y. Liang (2008), Trophic state, natural organic matter content, and disinfection by-product formation potential of six drinking water reservoirs in the Pearl River Delta, China, *J. Hydrol.*, *359*(1–2), 164–173.

Hua, F., T. F. Chen, and J. P. Lin (2003), Common cutgrass: Its characteristics of soil conservation and application on water-fluctuation belt at Xinfengjiang Reservoir, *Trop. Geogr.*, *23*(3), 214–217.

Jackson, L. J., T. L. Lauridsen, M. Søndergaard, and E. Jeppesen (2007), A comparison of shallow Danish and Canadian lakes and implications of climate change, *Freshwater Biol.*, *52*(9), 1782–1792.

Jin, X., Y. He, G. Kirumba, Y. Hassan, and J. Li (2013), Phosphorus fractions and phosphate sorption-release characteristics of the sediment in the Yangtze River estuary reservoir, *Ecol. Eng.*, *55*, 62–66.

Kirk, J. L., D. C. M. Muir, D. Antoniades, M. S. V. Douglas, M. S. Evans, T. A. Jackson, H. Kling, S. Lamoureux, D. S. S. Lim, and R. Pienitz (2011), Climate change and mercury accumulation in Canadian high and subarctic lakes, *Environ. Sci. Technol.*, *45*(3), 964–970.

Lafargue, E., F. Marquis, and D. Pillot (1998), Rock-Eval 6 applications in hydrocarbon exploration, production, and soil contamination studies, *Oil Gas Sci. Tech.*, *53*(4), 421–437.

Larsson, P., L. Okla, and G. Cronberg (1998), Turnover of polychlorinated biphenyls in an oligotrophic and a eutrophic lake in relation to internal lake processes and atmospheric fallout, *Can. J. Fish. Aquat. Sci.*, *55*(8), 1926–1937.

Li, L., J. D. Xu, and R. S. Cai (2002), Trends of sea level rise in the South China Sea during the 1990s: An altimetry result, *Chin. Sci. Bull.*, *47*(7).

Lin, Q. Q., L. M. Lei, and B. P. Han (2007), Cyanophyta in south subtropical reservoirs with different trophic levels, *Chin. J. Ecol.*, *7*, 10.

Liu, L. Y., J. Z. Wang, G. L. Wei, Y. F. Guan, C. S. Wong, and E. Y. Zeng (2012), Sediment records of polycyclic aromatic hydrocarbons (PAHs) in the continental shelf of China: Implications for evolving anthropogenic impacts, *Environ. Sci. Technol.*, *46*(12), 6497–6504.

Liu, Y. F., J. Q. Qin, and Y. S. Liang (2011), Analysis of aquatic ecosystem of Zeng Tang reservoir from virtuous cycle to eutrophication, *Guangdong Chem. Ind.*, *7*, 53.

Loring, D. H., and R. Rantala (1992), Geochemical analyses of marine sediments and suspended particulate matter, *Earth Sci. Rev.*, *32*, 235–283.

Louchouarn, P., L. J. Kuo, J. M. Brandenberger, F. Marcantonio, C. Garland, G. A. Gill, and V. Cullinan (2012), Pyrogenic inputs of anthropogenic Pb and Hg to sediments of the Hood Canal, Washington, in the 20th century: Source evidence from stable Pb isotopes and PAH signatures, *Environ. Sci. Technol.*, *46*(11), 5772–5781.

Ma, X. X., Y. Ran, J. A. Gong, and D. Y. Chen (2010), Sequential accelerated solvent extraction of polycyclic aromatic hydrocarbons with different solvents: Performance and implication, *J. Environ. Qual.*, *39*(6), 2072–2079.

Mai, B. X., J. M. Fu, G. Zhang, Z. Lin, Y. S. Min, G. Y. Sheng, and X. M. Wang (2001), Polycyclic aromatic hydrocarbons in sediments from the Pearl river and estuary, China: Spatial and temporal distribution and sources, *Appl. Geochem.*, *16*(11), 1429–1445.

Mai, B. X., H. M. Fu, G. Y. Sheng, Y. H. Kang, Z. Lin, G. Zhang, Y. S. Min, and E. Y. Zeng (2002), Chlorinated and polycyclic aromatic hydrocarbons in riverine and estuarine sediments from Pearl River Delta, China, *Environ. Pollut.*, *117*(3), 457–474.

Meyers, P. A. (1997), Organic geochemical proxies of paleoceanographic, paleolimnologic, and paleoclimatic processes, *Org. Geochem.*, *27*(5–6), 213–250.

Michelutti, N., H. J. Liu, J. P. Smol, L. E. Kimpe, B. E. Keatley, M. Mallory, R. W. Macdonald, M. S. V. Douglas, and J. M. Blais (2009), Accelerated delivery of polychlorinated biphenyls (PCBs) in recent sediments near a large seabird colony in Arctic Canada, *Environ. Pollut.*, *157*(10), 2769–2775.

Muir, D. C. G., A. Omelchenko, N. P. Grift, D. A. Savoie, W. L. Lockhart, P. Wilkinson, and G. J. Brunskill (1996), Spatial trends and historical deposition of polychlorinated biphenyls in Canadian midlatitude and Arctic lake sediments, *Environ. Sci. Technol.*, *30*(12), 3609–3617.

Outridge, P., G. Stern, P. Hamilton, J. Percival, R. McNeely, and W. Lockhart (2005), Trace metal profiles in the varved sediment of an Arctic lake, *Geochim. Cosmochim. Acta*, *69*(20), 4881–4894.

Outridge, P., H. Sanei, G. Stern, P. Hamilton, and F. Goodarzi (2007), Evidence for control of mercury accumulation rates in Canadian High Arctic lake sediments by variations of aquatic primary productivity, *Environ. Sci. Technol.*, *41*(15), 5259–5265.

Páez-Osuna, F., H. Bojorquez-Leyva, and J. I. Osuna-López (1991), Accumulation and distribution of phosphorus in sediments of the Gulf of California, *Mar. Min.*, *10*, 285–301.

Ran, Y., K. Sun, Y. Yang, B. Xing, and E. Zeng (2007), Strong sorption of phenanthrene by condensed organic matter in soils and sediments, *Environ. Sci. Technol.*, *41*(11), 3952–3958.

Ritchie, J. C., and J. R. McHenry (1990), Application of radioactive fallout cesium-137 for measuring soil erosion and sediment accumulation rates and patterns: A review, *J. Environ. Qual.*, *19*(2), 215–233.

Sanchez-Cabeza, J., and A. Ruiz-Fernández (2012), ^{210}Pb sediment radiochronology: An integrated formulation and classification of dating models, *Geochim. Cosmochim. Acta*, *82*, 183–200.

Sanei, H., L. D. Stasiuk, and F. Goodarzi (2005), Petrological changes occurring in organic matter from Recent lacustrine sediments during thermal alteration by Rock-Eval pyrolysis, *Org. Geochem.*, *36*(8), 1190–1203.

Shifrin, N. S., and S. W. Chisholm (1981), Phytoplankton lipids: Interspecific differences and effects of nitrate, silicate and light–dark cycles, *J. Phycol.*, *17*(4), 374–384.

Simcik, M. F., S. J. Eisenreich, K. A. Golden, S. P. Liu, E. Lipiatou, D. L. Swackhamer, and D. T. Long (1996), Atmospheric loading of polycyclic aromatic hydrocarbons to Lake Michigan as recorded in the sediments, *Environ. Sci. Technol.*, *30*(10), 3039–3046.

Skoog, A., and R. Benner (1997), Aldoses in various size fractions of marine organic matter: Implications for carbon cycling, *Limnol. Oceanogr.*, *42*(8), 1803–1813.

Stein, R., B. Boucsein, and H. Meyer (2006), Anoxia and high primary production in the Paleogene central Arctic Ocean: First detailed records from Lomonosov Ridge, *Geophys. Res. Lett.*, *33*, L18606, doi:10.1029/2006GL026776.

Stern, G., H. Sanei, P. Roach, J. Delaronde, and P. Outridge (2009), Historical interrelated variations of mercury and aquatic organic matter in lake sediment cores from a subarctic lake in Yukon, Canada: Further evidence toward the algal-mercury scavenging hypothesis, *Environ. Sci. Technol.*, *43*(20), 7684–7690.

Whelan, J. K., and C. L. Thompson-Rizer (1993), Chemical methods for assessing kerogen and protokerogen types and maturity, *Org. Geochem.*, 289–353.

Wu, F. C., L. B. Xu, Y. G. Sun, H. Q. Liao, X. L. Zhao, and J. Y. Guo (2012), Exploring the relationship between polycyclic aromatic hydrocarbons and sedimentary organic carbon in three Chinese lakes, *J. Soil. Sediment.*, *12*(5), 774–783.

Yang, H. D., D. R. Engstrom, and N. L. Rose (2010), Recent changes in atmospheric mercury deposition recorded in the sediments of remote equatorial lakes in the Rwenzori Mountains, Uganda, *Environ. Sci. Technol.*, *44*(17), 6570–6575.

Yunker, M. B., R. W. Macdonald, R. Vingarzan, R. H. Mitchell, D. Goyette, and S. Sylvestre (2002), PAHs in the Fraser River basin: A critical appraisal of PAH ratios as indicators of PAH source and composition, *Org. Geochem.*, *33*(4), 489–515.

Zakaria, M. P., H. Takada, S. Tsutsumi, K. Ohno, J. Yamada, E. Kouno, and H. Kumata (2002), Distribution of polycyclic aromatic hydrocarbons (PAHs) in rivers and estuaries in Malaysia: A widespread input of petrogenic PAHs, *Environ. Sci. Technol.*, *36*(9), 1907–1918.

Erratum

In the originally published version of this article, several instances of text contained errors. The following have since been corrected and this version may be considered the authoritative version of record.

In Section 2, second paragraph, "1 cm" was changed to "2 cm".

In Section 3.2, first paragraph, "0.81% to 3.38% in ZT core, from 0.88% to 3.4% in LA core, and from 0.47% to 1.64% in XFJ core" was changed to "0.78% to 3.38% in ZT core, from 0.88% to 4.3% in LA core, and from 0.47% to 1.76% in XFJ core".

In Section 3.2, first paragraph, "For ZT and LA cores, S1 and S2 values are respectively in the ranges of 0.15–1.31 mg HC/g and 0.21–1.32 mg HC/g, showing increasing trends from the bottom layers to the top sections." was changed to "For ZT and LA cores, S1 values are respectively in the ranges of 0.13–1.31 mg HC/g and 0.21–1.32 mg HC/g, while S2 values are respectively in the ranges of 1.10–8.38 mg HC/g and 1.47–9.45 mg HC/g, showing increasing trends from the bottom layers to the top sections."

In Section 3.2, third paragraph, "1.48 to 3.91 mg/g, 0.31 to 4.41 mg/g, and 0.56 to 1.62 mg/g" was changed to "1.94 to 5.36 mg/g, 0.51 to 6.4 mg/g, and 0.83 to 2.56 mg/g".

In Section 3.3, first paragraph, "71–376 ng/g" was changed to "69—376 ng/g".

In Section 3.3, first paragraph, "174 ng/g, 205 ng/g, and 172 ng/g" was changed to "167 ng/g, 197 ng/g, and 179 ng/g".

In Section 4.1, second paragraph, "OI" was changed to "OIRE6" in four instances.

In Section 4.1, second paragraph, "375—837 mg" was changed to "375—883 mg".